# GEOSTATISTICAL MODELING OF SEISMIC ACTIONS ON THE STRUCTURAL COMPONENTS OF THE SAN BENEDETTO ROAD TUNNEL, ITALY

MASSIMO GUARASCIO, ANGELO LIBERTÀ, DAVIDE BERARDI,
EMIN ALAKBARLI & MARA LOMBARDI
Sapienza University of Rome, Italy

ABSTRACT

The Italian legislation requires determining the project seismic actions and to carry out the dynamic stability verification of the structural elements of a building or road infrastructure on the base of the seismic hazard curve of the construction site. The geographic density of the available seismic data requires the best use of existing data and above all not introducing phenomenological assumptions and unverified information into the survey. This article proposes an investigation protocol that integrates the multivariate statistical analysis methodologies already used to determine the seismic shaking attenuation with more efficient and versatile geostatistical methodologies for a more realistic estimate of non-stationary parameters. The application of the new investigation protocol to the earthquakes that occurred in Italy in 2016 made it possible to detect and resolve three fundamental aspects of seismic modeling: (i) the recorded data highlight the presence of a directional anisotropy of the arrival time and the value of the acceleration peak on the ground which led to the introduction of a non-Euclidean metric in seismic modeling; (ii) the presence and measurement of the geographical continuity of the irregular variations between data pairs attributable to the heterogeneity of the rock formations and outcropping soils; (iii) the need for an experimental measure of the estimate uncertainty for an objective evaluation of the applied numerical estimator. This last result made it possible to evaluate the gain in terms of accuracy of the estimate performed with the local geostatistical estimator. The article presents the estimate of the arrival time and the peak value of the vertical ($PGA_V$) and maximum horizontal ($PGA_H$) component of the acceleration of the vibrational movements of the rock around the San Benedetto tunnel during the Norcia earthquake. The maximum estimated values of $PGA_V$ and $PGA_H$ are around the section of the tunnel damaged by the earthquake.

*Keywords: earthquake, geostatistics, Universal CoKriging, seismic first-guess, risk, analysis, road tunnel, seismicity.*

## 1 INTRODUCTION

The Italian legislation (NTC 2018) limits the design of buildings and road infrastructures (viaducts, bridges, tunnels, etc.) to the seismic hazard of the construction site. The seismic actions of the project must be determined on the hazard curve by identifying the accelerations on the ground whose return times or the probabilities of exceeding during the life of the building are prescribed by the legislation and referred to the operating limit states, life protection and collapse of the building or infrastructure. In most cases, the centenary historical series of earthquakes that occurred in the seismogenetic area and the seismic monitoring data recorded during the most recent earthquakes are the only information available to plot the probability curves of the accelerations perceived by the building or infrastructure for future earthquakes in the geographic area of the construction site.

The limited number of data makes to use efficient objective methods of analysis and to not introduce into the seismic investigation phenomenological assumptions and unverified information. To this end, the authors propose an investigation protocol to perform an objective and verifiable estimate of the non-stationary ground-motion parameters and to draw the anisotropic ground-motion attenuation diagrams using at best the data recorded by a

WIT Transactions on The Built Environment, Vol 214, © 2022 WIT Press
www.witpress.com, ISSN 1743-3509 (on-line)
doi:10.2495/SSR220021

seismic monitoring network. Lithological data of rock formations and soils outcropping can be used if georeferenced and homogeneously detected. Below are the six phases of the seismic investigation:

(i) identify data recorded from the accelerometer stations the local main directions of seismic oscillations during earthquake and the local maximum ground shaking intensity (multivariate-statistical analysis);
(ii) identify the function of the geographic seismic patterns consistent with the theory of elastic wave propagation and the georeferenced seismic available data (first-guess function);
(iii) determine the geographic continuity model of the ground motion parameters to be estimated (statistical inference of the variogram function);
(iv) estimate the ground motion parameters in the station points using the best available data and the topographic model of the investigation area (cross-validation of no stationary multivariate geographical estimator);
(v) use the validated estimator to estimate the ground motion parameters in any geographical point using the best available data and the topographic model of the investigation area;
(vi) starting from the estimated seismic data at the nodes of a georeferenced grid, mark the directional attenuation profiles of the ground motion parameters of interest.

The above investigation protocol was applied to estimate, at the nodes of a 500 × 500 $m^2$ georeferenced grid, the arrival time and the value of the peak of the horizontal ($PGA_H$) and vertical ($PGA_V$) component of ground acceleration of the four earthquakes that occurred in 2016 in the central Italy: Accumoli (24 August 2016), Amatrice (26 August 2016), Castelsantangelo sul Nera (26 October 2016) and Norcia (30 October 2016).

The investigations carried out on the four earthquakes revealed three fundamental results not found in the scientific literature of the sector. Around the area of the maximum ground motions (epicentral area) the geographic pattern of the ground motion parameters is approximated by a continuous function (first-guess seismic) which is defined by the product of the geometric attenuation equation of an elastic wave emitted by a point source and the inelastic attenuation equation [1]. For each earthquake of 2016, the optimal adjustment of the *FgS* function obtained by minimizing the squares of the seismic residuals calculated as the difference between the PGA at the station points and the values of the *FgS* function at the same points, presents a directional anisotropy. This led to the modify the shape of the geometric attenuation equation and of the inelastic attenuation equation, introducing a non-Euclidean spatial metric for the first time in seismic modeling.

The second result is the measurement of the geographical continuity of the two seismic variables treated (arrival time and value of the PGA). This geographical property is likely inherited from the continuity of the lithological characteristics of the rock formations and surface soils crossed by the volume seismic waves (waves P and S) and by the surface seismic waves. More or less large volumes of rock with homogeneous or slightly variable lithological characteristics are in contact with volumes of rock with greater spatial variability or with different lithological characteristics. The average extension of the lithological discontinuities determines the geographical variability of the data recorded by the accelerometric stations.

This leads to the rejection of the hypothesis of random distribution of local seismic variations and, although locally the seismic variations are irregular, the average of the squared differences of the ground motion parameters recorded in two geographical points tends to zero when the distance between the points tends to zero.

The correlation between lithological characteristics and PGA probably will be found in other ground motion parameters such as the spectral parameters of the accelerograms (SA)

and the seismic indicators of engineering interest: Arias Intensity Index and Cosenza–Manfredi Index [2], which can then be analyzed with the proposed investigation protocol.

The identified *FgS* functions are compatible with the theory of propagation of inelastic waves within a rock model whose lithological properties are likely a spatial average of the lithological properties of the rock volumes crossed by the seismic waves. The more the rock formations are heterogeneous, the higher is the geographic variability of the residues of the FgS function. The geographic variability of seismic residues is proportional to the lithological heterogeneity of the volumes of rock crossed by the seismic waves. For the authors, the variance of local dispersion of seismic residues is a correct indicator of the complex and undetectable geometry of the stratigraphic surfaces and the heterogeneity of rocks and soils outcropping [3]. And the origin of the local indeterminacy of ground shaking intensity is the unbridgeable difference between the amount of information needed to solve the complexity of the geostratigraphic system with sufficient approximation and the seismic information contained in the available data. The local indeterminacy of the estimate is quantified by the variance of the estimation error, which is calculated by the same no-stationary geostatistical estimator (Universal CoKriging (UCoK) with external drift). For each data detected around the point to be estimated, the UCoK calculates a weight coefficient that depends on: (i) the local function of geographical continuity of the seismic variable; (ii) geometry of the seismic monitoring network; (iii) position of the accelerometric stations with respect to the point to be estimated. Therefore the local indeterminacy of the estimate does not depend only on the distance of the point to be estimated from the epicentral area, as predicted by the logarithmic estimator proposed by Campbell [1] and subsequently applied by Boore et al. [4] and by Sabetta and Pugliese [5] but, as aforementioned, also from the number and position of the data collected around each point to be estimated.

The third result that emerged from the survey is the measurement of the gain in terms of accuracy of the local estimate obtained with the geostatistical estimator compared to the estimate obtained with the *FgS* function. The improvement in the estimate is measured by the difference between the variance of the seismic residuals from the *FgS* function in the station points and the variance of the local estimation error in the same station points. In phase IV of the seismic survey, the UCoK estimator is used to calculate the ground-motion parameters in the station points, eliminating the station data to be estimated from the calculation each time. In each station point and for each ground motion parameters are therefore available: (i) the data detected (data known only in the station points); (ii) the seismic residue of the datum detected by the *FgS* function (iii) the datum estimated with the UCoK estimator; (iv) the estimation error committed by the UCoK (difference between true data and estimated data; (v) variances of the estimation error calculated by the same UCoK estimator. For each of the four Italian earthquakes it was found that:

(i) the *FgS* function and the UCoK are both unbiased estimators (the average of the seismic residues and the average of the estimation errors are close to zero);
(ii) the variance of dispersion of the estimation errors committed with the UCoK was always lower than the variance of dispersion of the seismic residuals referred to the function of *FgS*;
(iii) the variance of the estimation error calculated by the UCoK is very close to the variance of dispersion calculated on the real estimation errors.

It follows that the function of *FgS* is a first approximation of the attenuation of ground motions and cannot be assumed a priori as the prediction equations of ground shaking intensity as proposed by Campbell [6], Boore et al. [4] and Sabetta and Pugliese [5].

The paper show how estimate the arrival time and the peak value of the vertical ($PGA_V$) and horizontal ($PGA_H$) component of the acceleration of the rocks around the San Benedetto tunnel during the Norcia earthquake (30 October 2016)

## 2 GEOSTATISTICAL FRAMEWORK

Initially, geostatistics was developed to estimate mineral deposits [7] but the same methodologies were found to be valid and therefore currently applied in many fields of earth sciences (hydrogeology, meteorology, oceanography, geochemistry, environmental control, soil science, etc.). The basis of geostatistical methodologies is the observation that some natural phenomena have a geographical evolution and local states are closely related to their position. This typology of phenomena has been defined as "regionalized phenomena" and consequently the variables that describe them are defined as "regionalized variables" (V.R.) [8].

The states assumed by a V.R. at points x of a geographic domain are represented by a function *z(x).* Locally, the *z(x)* function is highly irregular and the variations from one point to another are often unpredictable, while over greater distances the function is more continuous and shows the structural characteristics of the physical phenomenon that underlies the observed regionalized phenomenon. This feature suggested developing the function *z(x)* into a sum of two functions; the first, indicated by *m(x),* which represents the geographical trend of the regionalized phenomenon and the second, indicated by *y(x),* which reflects the irregular local variations of the observed phenomenon: $z(x) = m(x) + y(x)$. As they are defined, the two components are statistically independent.

This double aspect is found in numerous geophysical and geochemical variables such as: temperature of the layer of atmosphere in contact with the earth's surface (temperature decreases with latitude and topographical altitude), concentration of pollutants in the soil (concentration increases near an oil plant) or vibrations of the ground following a seismic event (vibrations of the ground decrease with the distance from the epicentral area of the earthquake).

The irregular geographical evolution of natural phenomena has suggested the conceptual choice of considering the R.V. z(x) of the realizations of Random Functions (R.F.) Z(x) defined on a precise geographical domain D of the Euclidean space $\mathbb{R}^n$. The function m(x) represents at each point x the expected value of the R.F. Z(x): $E|Z(x)|=m(x)$. The residual Y(x) of the R.F. Z(x) is a locally stationary R.A. with $E|Y(x)|=0$ and covariance $Cov|Y(x_1), Y(x_2)| = E|Y(x_1)\ Y(x_2)|<\infty$. In the study of the natural phenomena described by several V.R. related, information on the geographical structure of the R.F. $Z_i(x)$ e $Z_j(x)$ is developed by the variograms and cross-variograms of the R.F. of the residuals $Y_i(x)$ and $Y_j(x)$:

$$\gamma_{i,j}(\vec{h}) = \frac{1}{2}\boldsymbol{E}|[(Y_i(x+\vec{h}) - Y_i(x)][(Y_j(x+\vec{h}) - Y_j(x)]|. \quad (1)$$

Universal CoKriging with external drift is a specialization of Universal CoKriging (UCoK) applied when the functions that describe the geographic pattern of the regionalized variables studied (external drift) are known. UCoK is widely used in earth sciences to map geophysical or geochemical variables such as the minimum and maximum air temperature or the concentration of metals or pollutants in the soil. The UCoK estimator is numerically equivalent to a multivariate geographic regression conditional on the directional variogram and cross-variogram functions of the target variable and the auxiliary variables. The estimate of the target variable $Z_o$ at point x is obtained from the linear combination (weighted average) of the data of the target variable $Z_o$ and the auxiliary variables $Z_i$ which have a geographical correlation with the target variable.

The universal CoKriging with external drift assumes that (i) the geographic patterns of the R.F. objective and the R.F. auxiliaries are in every point of the geographic domain equal to $E|Z_i(x)| = \sum_{l=0}^{L} a_{i,l}\, f_i^l(x)$; (ii) for each pair of points in the geographic domain, the mean of the squared differences of the R.F. and the average of the product of the difference between two R.F. are determined by the variogram and cross-variogram model.

For each point to be estimated the estimation weigh coefficients of the data $\lambda_{k,i}$ are obtained by setting the following conditions:

(i) average estimation error of the zero target variable: $\boldsymbol{E}|[(Z_0^*(x) - Z_0(x)]| = 0$
The condition of unbiased for the UCoK estimator becomes: $\boldsymbol{\lambda}_i^T\, \boldsymbol{F}_{i,l} = \delta_{i,l}\, \boldsymbol{f}_l^T$

(ii) variance estimator error of the minimum target variable:

$$\boldsymbol{Var}|[(Z_0^*(x) - Z_0(x)]| = 2\, \sum_{\boldsymbol{i}} \boldsymbol{\lambda}_i^T\, \boldsymbol{\Gamma}_{i,0} - \sum_{\boldsymbol{i}} \sum_{\boldsymbol{j}} \boldsymbol{\lambda}_i^T\, \boldsymbol{\Gamma}_{i,j}\, \boldsymbol{\lambda}_j = \text{min.}$$

## 3 NORCIA EARTHQUAKE OF 30 OCTOBER 2016

This section presents the results of the seismic survey of the Norcia earthquake of 30 November 2016 (seismogenic zone of the Central Italian Apennines) performed to determine the shaking intensity that the San Benedetto tunnel underwent during the seismic event. The UCoK estimator was used to estimate the seismic variables time of arrival and peak value of the vertical ($PGA_V$) and maximum horizontal ($PGA_H$) component of the acceleration of the vibrational movements of the rock. The two seismic variables were estimated at the nodes of a three-dimensional grid with a distance between the nodes of 13.5 m in the direction of the longitudinal axis of the tunnel and 27.0 m in the transverse plane. The extension of the grid is 4,117.5 m in the direction of the longitudinal axis of the tunnel and 216 × 216 $m^2$ in the transverse plane.

The basic data used to estimate the 2 seismic variables are: (i) the seismograms recorded by the accelerometric stations; (ii) the geographic coordinates and the altitude of the accelerometric stations; (iii) the geo-referenced altimetric model with 500 m cells (DTM); (iv) the geographical coordinates and the height of the grid nodes around the San Benedetto tunnel.

### 3.1 Local dimensional ground motions seismic.

The effects and the failure of the structural elements of a building caused by seismic motions depend both on the intensity of the shaking and on the directions of oscillation of the ground during an earthquake. For the purpose of verifying the dynamic stability of the structural elements of a building or road infrastructure it is useful to know the directions of the principal axes of a 3D-orthogonal system along which the component of ground motion have maximum, minimum and intermediate values of variance and have zero values of covariance. The methodology proposed by Pazien and Watabe [9] was used to determine, starting from the accelerograms recorded by the stations of the seismic monitoring network of Central Italy, the local directions of the three main axes of ground motions during the Norcia earthquake. The method used usually to compute the principal axes is by diagonalized the covariance matrix of ground accelerograms recorded along the instrument axes:

$$\boldsymbol{C}(t) = \begin{vmatrix} c_{x,x} & c_{x,y} & c_{x,z} \\ c_{y,x} & c_{y,y} & c_{y,z} \\ c_{z,x} & c_{z,y} & c_{z,z} \end{vmatrix} \tag{2}$$

where $c_{i,j}(t) = E\left|a_i(t)\, a_j(t)\right|$ and $a_i(t)$ are random functions which represented accelerograms recorded along east–west, north–south and vertical direction. The time interval is 0.005 seconds.

The directions of the principal axes are the eigenvectors computed through the use of the covariance matrix $\boldsymbol{C}(t)$ and the principal variances are the corresponding eigenvalues. It has been verified that the time-correlation of the accelerations $a_i(t)$ is zero after 0.01 seconds and in the same time-intervals the average of the accelerations is close to zero.

Since ground motions are non-stationary over time a moving window technique is applied to analyze the time-dependent characteristic of the direction of principal axes. The eigenvalues and eigenvectors are calculated on disjoint intervals of 0.25 seconds using the 200 data recorded in the interval of one second centered in the target interval.

In the fifteen accelerometric stations closest to the epicentral area of the Norcia earthquake (2016), the main axis with the least variance is sub-vertical in the interval time of maximum seismic shaking (Fig. 1). In the same interval the other two principal axes are naturally sub-horizontal. For these two axes the direction is not always constant over time. For the axes of major and intermediate values of variance, a statistically prevalent direction was not found. Although for a few stations, such as that of Forche Canapina (identified by the FCC code), a prevailing direction can be identified (Fig. 1).

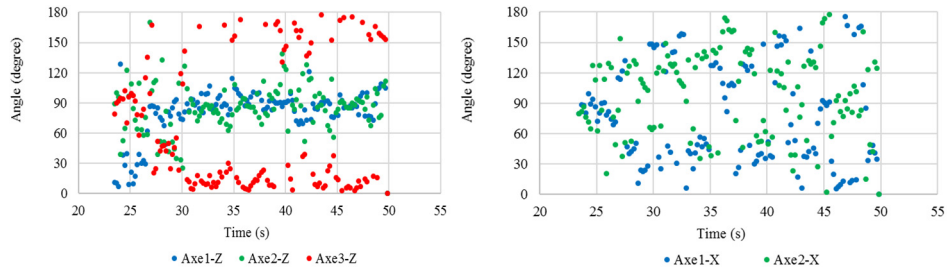


Figure 1: Scatter diagrams: Angle between principal axes and the two direction vertical and east–west (FCC station).

The scatter-diagram of the first graph in Fig. 1 shows the angles that the main axes form with the vertical direction of the FCC station. The direction of the axe with minimum value of variance is parallel to the vertical direction (red dots) while the other two main axes are orthogonal to the vertical direction. The second graph in Fig. 1 shows the angles that the axes with maximum and intermediate values of variance form with the east–west direction. The prevailing direction of the main axes 1 and 2 close to 45° and 135° respectively can be seen from the scatter diagram of second graph in Fig. 1.

### 3.2 First-guess of seismic variables

The first-guess fields of the two seismic variables are described by continuous mathematical functions defined at all points of the geographical survey domain.

In geostratigraphic systems, the regionalization of the ground motion parameters differs from the geographical pattern predicted from the theory of propagation of anelastic waves in a homogeneous material due to the heterogeneity of the rock formations crossed and the complex geometry of the fault systems and the stratigraphic contacts between lithological units:

- the different propagation velocity of seismic waves in rocks deform the geometry of the wave surfaces with consequent directional variations of the geometrical attenuation;
- moreover, irregular local variations of the seismic oscillations are a consequence of the different anelastic behavior of the rocks. A part of the energy carried by the seismic waves is continuously and irregularly dissipated by friction (anelastic attenuation).

Despite this, the data of the seismograms recorded by the accelerometric stations show good consistency with the PGA geographic pattern (Fig. 2) and the arrival time of the acceleration peak (Fig. 3) described by the functions of *FgS*.

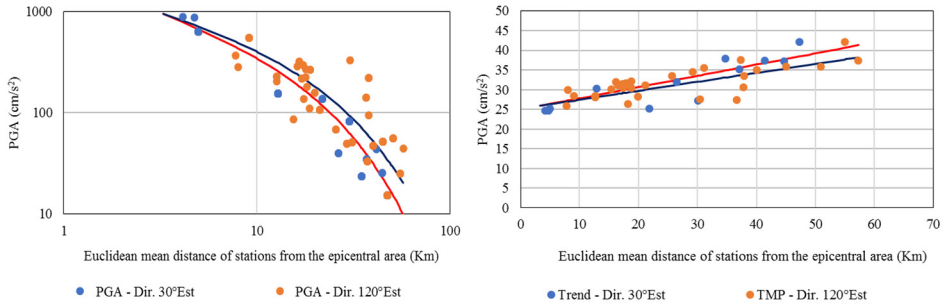


Figure 2: First-guess of $PGA_V$ and arrival time in Euclidean distance.

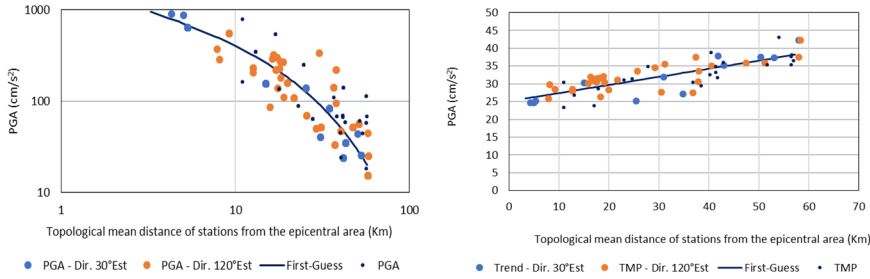


Figure 3: First-guess of $PGA_V$ and arrival time in topological distance.

The scatter-diagrams of the arrival time and the value of the acceleration peak on the ground recorded by the stations in the direction orthogonal to the Apennine axis (probable fault direction) (red points) are mainly arranged in the lower part ($PGA_V$) and in the high (arrival time) of the cloud. In the graphs, the abscissa axe indicates the Euclidean mean distance from the epicentral area. This directional anisotropy also emerged in the numerical simulations performed to estimate the coefficients of the *FgS* function.

*First-guess function of the arrival time of the acceleration peak*

$$f_t(x) = a_t(x_0) - b_t(x_0)\,\overline{r}_0(x), \tag{3}$$

where $x_0$ identifies the pair of coordinates of the center of gravity of the epicentral area of the seismic event; $a_t(x_0)$ and $b_t(x_0)$ are the coefficients of the regression line; $\overline{r}_0(x)$ is the

average topological distance of the x coordinate point from the epicentral area (average of the topological distances between the point and the points of the circle with a radius of 5 km centered at the point $x_0$) [8].

*First-guess function of the peak ground acceleration (PGA)*

$$f_p(x) = \frac{a_p(x_0)}{\sqrt{\overline{r}_0(x)}}\, e^{-b_p(x_0)\,\overline{r}_0(x)} \tag{4}$$

where: $x_0$ identifies the pair of coordinates of the center of gravity of the epicentral area of the seismic event; $a_p(x_0)$ and $b_p(x_0)$ are the coefficients of the FgS function, which it describes the geographical pattern of the PGA; $\overline{r}_0(x)$ is, as for the seismic variable time of arrival, the average topological distance of the point of coordinates x from the epicentral area.

In the two first-guess functions the topological distance between any pair of points x' and x" is defined as: $d(x', x'') = \sqrt[2]{\boldsymbol{X}^T \boldsymbol{H}\, \boldsymbol{X}}$ where $\boldsymbol{X} = (x_1'' - x_1', x_2'' - x_2')^T$ is the difference vector of the metric coordinates of the two points, and $\boldsymbol{H} = \boldsymbol{\psi}\, \boldsymbol{M}\, \boldsymbol{\psi}^T$ is the product of the rotation matrix of the cartesian reference system and of the metric tensor M used to introduce in the first-guess functions the directional anisotropy of the seismic variables:

$$\boldsymbol{M} = \begin{vmatrix} (1+\alpha)^2 & 0 \\ 0 & 1 \end{vmatrix}. \tag{5}$$

The coefficient α is the expansion factor of the metric coordinates of the Cartesian axis orthogonal to the Apennine alignment (oriented at 35° east).

The position of the epicentral area must be compatible with the geographic pattern described by the $m_p(x)$ function and with the PGA data at the points of the accelerometric stations.

To calculate the coefficients of the *FgS* function of the PGA, a Monte Carlo simulation is performed, which consists of N random extractions of the inelastic damping coefficient, of the angle between the direction of greatest geometric attenuation and the East direction and of the coefficient a of the metric tensor M for each node of the 500 × 500 m$^2$ grid. The numerical values extracted are compatible with the seismic phenomenon to be modeled. For each extraction, the coefficient ap is determined (adjustment factor to the existing seismic data) which minimizes the difference between the PGA data at the station points and the following function (multivariate geographic regression):

$$m_p(x) = c_0 + c_q q(x) + \frac{a_p(x_0)}{\sqrt{\overline{r}_0(x)}}\, e^{-b_p(x_0)\,\overline{r}_0(x)} \tag{6}$$

where $x_0$ is the coordinate of the grid node and *q(x)* is the topographic elevation at the *x* coordinate point. The coefficient $a_p$ is calculated as the weighted average of the PGA data around the node to be estimated $a_p(x_0) = \sum_{i=1}^{n} \lambda_{0,i}\, z(x_i)$ and the weight coefficients $\lambda_{0,i}$ are the solutions of the following linear system:

$$\begin{cases} \boldsymbol{I}\, \boldsymbol{\lambda}_l + \boldsymbol{F}\, \boldsymbol{\mu} &= 0 \\ \boldsymbol{F}^T\, \boldsymbol{\lambda}_l &= \delta_{k,l} \end{cases} \tag{7}$$

where $\boldsymbol{I}$ is the identity matrices *nxn*; $\boldsymbol{F}$ is the *nx3* matrix of the values of the development terms of $m_p(x)$ in the n observation points; $\boldsymbol{\mu}$ is the vector of the three Lagrange multipliers and $\delta_{k,l}$ is the operator to set equal to 1 the *k*-th term of the coefficient to be estimated.

In the scatter diagrams the arrangement of the points representing the arrival time and the value of the ground acceleration peak recorded by the 65 seismic stations is consistent with

the inelastic wave propagation theory represented by the *FgS* function (continuous curve). In the graphs, the abscissa axe indicates the topological average distance from the epicentral area $d(x', x'') = \sqrt[2]{\boldsymbol{X}^T \boldsymbol{H}\, \boldsymbol{X}}$.

### 3.3 Estimation by Universal CoKriging

The validated UCoK estimator was used to estimate the arrival time and the peak value of the vertical and horizontal components of the ground acceleration in the area of San Benedetto tunnel. The estimation was performed using data of ten accelerometric station near the tunnel (Fig. 4) and first-guess functions of both seismic variables, variogram and cross-variogram models and digital terrain model (DTM).

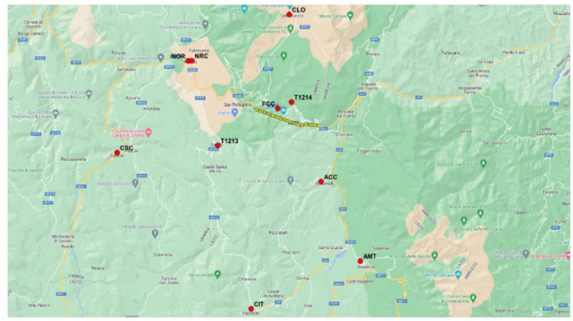


Figure 4: Position of the ten accelerometric stations used to estimate the two seismic variables at the nodes of the San Benedetto tunnel grid (in yellow the tunnel).

The estimate of the target variable $Z_0$ at grid-node x is obtained from the linear combination (weighted average) of the data of the target variable $Z_0$ and the auxiliary variable $Z_i$ which have a geographical correlation with the target variable:

$$Z_0^*(x) = \sum_{k=0}^{m} \sum_{i=1}^{n} \lambda_{k,i}\, Z_k(x_i), \tag{8}$$

where $\lambda_{0,i}$ are the weight coefficients of the target variable and $\lambda_{k,i}$ are the weight coefficients of the auxiliary variable (index k>0) and $x_j$ are the coordinates of the n observation points ($x_j$ represents the pair of metric coordinates necessary to locate the *i*-th point in the geographic domain).

For each node of grid to be estimated the coefficients $\lambda_{k,i}$ are obtained from the following linear system (9):

$$\begin{cases} \sum_{k=0}^{m} -\boldsymbol{\Gamma}_{i,j}\, \boldsymbol{\lambda}_j \;+\; \boldsymbol{F}_i\, \boldsymbol{\mu}_i = -\boldsymbol{\Gamma}_{i,0} & i = 0 \ldots m \\ \boldsymbol{F}_i^T\, \boldsymbol{\lambda}_i = \boldsymbol{f}_{l,0}\, \delta_{i,l} & i = 0 \ldots m, \end{cases} \tag{9}$$

where $\boldsymbol{\Gamma}_{i,j}$ are the *n*x*n* matrices of variograms or cross-variograms of F.A. $Z_i$ and $Z_j$between each observation points pair; $\boldsymbol{F}_{i,l}$ are the nxL matrix of the values of the first-guess functions at the observation points; $\boldsymbol{\Gamma}_{i,0}$ are the vectors of the variograms and cross-variograms between the point to be estimated (target-point) and the observation points of the F.A. to be estimated with the F.A. $Z_i$ and $\boldsymbol{f}_{l,0}\, \delta_{i,l}$ are the vectors of the values of the first-guess function of the V.R. to be estimated and sold set to zero the conditions of unbiased of the V.R. auxiliaries.

The variance of the estimation error or cokriging variance is given by:

$$\sigma_{CK}^2 = \sum_{k=0}^{m} \boldsymbol{\lambda}_k^T \boldsymbol{\Gamma}_{k,0} + \boldsymbol{\mu}_l^T \boldsymbol{f}_{i,0}, \quad (10)$$

where $\boldsymbol{\lambda}_{i,0}$ are the vectors of the F.A. $Z_i$ and $\boldsymbol{\mu}_{i,0}$ are the vectors of the Lagrange parameters associated with the F.A. $Z_i$. The variance of the estimate quantifies the uncertainty of the estimate and, as defined, depends: (i) on the number of observation points; (ii) on the geometry of the observation points; (iii) on the position of the observation points with respect to the point to be estimated and (iv) on the local variability of the V.R. treated.

The value and variance of the two seismic variables were estimated in each node of grid.

In Table 1 the target variable is the PGA and the estimated value is the standard deviation of the estimation error and the relative estimation error. Table 2 shows the results of the estimation for the target arrival time variable. The two tables lists the ten accelerometric stations and for each one the distance from the estimated node and the weight coefficients of the target variable and the auxiliary variable are indicated. Tables 3 and 4 show the estimation of PGA and arrival time in some point of the tunnel.

Table 1: Estimation of the vertical acceleration peak (PGA).

| Prg | ID station | Altitude (m) | Distance (Km) | PGAv (cm/s$^2$) | Arrival time (s) | CoKriging Weight PGA | CoKriging Weight Arrival time |
|---|---|---|---|---|---|---|---|
| 1 | FCC | 1553 | 1.267 | 893.50 | 24.74 | 1.4055 | -14.3869 |
| 2 | T1214 | 1490 | 2.649 | 632.91 | 25.18 | 0.0207 | 22.0470 |
| 3 | CLO | 1456 | 8.978 | 782.02 | 23.33 | -0.0651 | -0.4670 |
| 4 | NRC | 616 | 8.130 | 367.53 | 25.89 | -0.1470 | -2.8061 |
| 5 | NOR | 662 | 8.400 | 283.36 | 29.87 | -0.0626 | -4.2986 |
| 6 | CSC | 683 | 14.078 | 155.84 | 30.32 | 0.0137 | -0.7633 |
| 7 | T1213 | 860 | 5.214 | 868.89 | 24.67 | -0.0219 | 1.0059 |
| 8 | CIT | 873 | 17.512 | 135.27 | 28.62 | 0.0409 | 2.2989 |
| 9 | ACC | 922 | 8.062 | 546.90 | 28.42 | -0.1969 | -2.6447 |
| 10 | AMT | 950 | 15.899 | 317.82 | 31.17 | 0.0127 | 0.0148 |
| | **Distance from epecentral area** | | **1.625** | | | **1.0000** | **0.0000** |
| | | | **Estimated PGAv** | **1011.37** | | | |
| | | | **DevStandard error** | **145.88** | | | |
| | | | **Relative error (%)** | **14.42** | | | |

Table 2: Estimation of the arrival time of the vertical acceleration peak.

| Prg | ID station | Altitude (m) | Distance (Km) | PGAv (cm/s$^2$) | Arrival time (s) | CoKriging Weight PGA | CoKriging Weight Arrival time |
|---|---|---|---|---|---|---|---|
| 1 | FCC | 1553 | 1.267 | 893.50 | 24.74 | -0.0006 | 0.8439 |
| 2 | T1214 | 1490 | 2.649 | 632.91 | 25.18 | 0.0016 | 0.1690 |
| 3 | CLO | 1456 | 8.978 | 782.02 | 23.33 | 0.0001 | -0.0493 |
| 4 | NRC | 616 | 8.130 | 367.53 | 25.89 | -0.0005 | -0.0444 |
| 5 | NOR | 662 | 8.400 | 283.36 | 29.87 | -0.0004 | -0.0316 |
| 6 | CSC | 683 | 14.078 | 155.84 | 30.32 | 0.0000 | -0.0291 |
| 7 | T1213 | 860 | 5.214 | 868.89 | 24.67 | -0.0005 | 0.2067 |
| 8 | CIT | 873 | 17.512 | 135.27 | 28.62 | 0.0002 | 0.0210 |
| 9 | ACC | 922 | 8.062 | 546.90 | 28.42 | 0.0001 | -0.0847 |
| 10 | AMT | 950 | 15.899 | 317.82 | 31.17 | 0.0000 | -0.0015 |
| | **Distance from epecentral area** | | **1.625** | | | **0.0000** | **1.0000** |
| | | | **Estimated arrival time of PGA** | | **24.17** | | |
| | | | **DevStandard error** | | **1.61** | | |
| | | | **Relative error (%)** | | **6.66** | | |

Table 3: Estimation of the vertical acceleration peak (PGA).

| Estimated point | Epicentral distance (Km) | Estimate PGA ($cm/s^2$) | DevStandard error ($cm/s^2$) | Relative error (%) |
|---|---|---|---|---|
| West portal area (San Pellegrino di Norcia) | 1.679 | 1013.12 | 147.06 | 14.52 |
| Tunnel lining segment at point 906,5 m | 1.622 | 1011.69 | 146.22 | 14.45 |
| Tunnel lining segment at point 920 m | 1.625 | 1011.37 | 145.88 | 14.42 |
| Tunnel lining segment at point 933,5 m | 1.629 | 1010.97 | 145.45 | 14.39 |
| East portal area (Capodacqua) | 3.886 | 776.01 | 105.52 | 13.60 |

Table 4: Estimation of the arrival time of the vertical acceleration peak.

| Estimated point | Epicentral distance (Km) | Estimate arrival time of PGA (s) | DevStandard error (s) | Relative error (%) |
|---|---|---|---|---|
| West portal area (San Pellegrino di Norcia) | 1.679 | 24.05 | 1.69 | 7.03 |
| Tunnel lining segment at point 906,5 m | 1.622 | 24.17 | 1.62 | 6.70 |
| Tunnel lining segment at point 920 m | 1.625 | 24.17 | 1.61 | 6.66 |
| Tunnel lining segment at point 933,5 m | 1.629 | 24.17 | 1.61 | 6.66 |
| East portal area (Capodacqua) | 3.886 | 25.78 | 1.42 | 5.51 |

Fig. 5 shows the growth of the vertical acceleration peak from east to west with a maximum of 1,027.13 $cm/s^2$ at the level of the tunnel floor. In correspondence with the breaking segment of the road surface, the vertical acceleration peak was 1,013.17 $cm/s^2$.


Figure 5: Geostatistical estimate of the vertical acceleration peak in the nodes of the 3D grid 13.5 m in the direction of the longitudinal axis of the San Benedetto tunnel (yellow dots) and 27.0 m in the transverse vertical plane.

## 4 CONCLUSIONS

The results obtained on the four earthquakes of 2016 show how the lithological heterogeneity and the succession of rock formations and outcropping soils determined the geographical directional attenuation of the peaks of the horizontal and vertical components of the ground acceleration. This correlation between lithological characteristics and PGA will likely be found in other ground motion parameters such as the spectral parameters of the accelerograms (SA) and the seismic indicators of engineering interest.

## REFERENCES

[1] Campbell, K.W., Strong motion attenuation relations: A ten-year perspective. *Earthquake Spectra*, **1**(4), pp. 759–804, 1985. DOI: 10.1193/1.1585292.
[2] Cosenza, E. & Manfredi, G., Damage indices and damage measures. *Progress in Structural Engineering and Materials*, **2**, pp. 50–59, 2000.
[3] Guarascio, M., Libertà, A., Berardi, D., Di Benedetto, E. & Lombardi, M., Seismic geostatistics application to the territorial infrastructure resilience and sustainability. *Transactions on The Built Environment*, vol. 206, WIT Press: Southampton and Boston, 2021.
[4] Boore, D.M., Joyner, W.B. & Fumal, T.E., Estimation of response spectra and peak accelerations from western North American earthquakes: An interim report, Part 2, U.S. Geol. Surv. Open-File Rep. 94-127, 40 pp, 1994.
[5] Sabetta, F. & Pugliese, A., Estimation of response spectra and simulation of nonstationary earthquake ground motions. *Bulletin of the Seismological Society of America*, **86**(2), pp. 337–352, 1996. DOI: 10.1785/BSSA0860020337.
[6] Campbell, K.W., Strong motion attenuation relations. *International Handbook of Earthquake and Engineering Seismology, Part B*, pp. 1003–1012, 2003.
[7] Guarascio, M., Huybrechts, C.J. & David, M., Advanced Geostatistics in the Mining Industry. *Proceedings of the NATO Advanced Study Institute*, 13–25 Oct., Istituto di Geologia Applicata of the University of Rome, Italy, 1975.
[8] Matheron, G., Random sets theory and its applications to stereology. *Journal of Microscopy*, **95**, pp. 15–23, 1972. DOI: 10.1111/j.1365-2818.1972.tb03708.x.
[9] Pazien, J. & Watabe, M., Characteristics of 3-dimensional earthquake ground motions. *Earthqu. Eng. Struct. Dyn*., **3**, pp. 365–373, 1975.